General Disclaimer

One or more of the Following Statements may affect this Document

- This document has been reproduced from the best copy furnished by the organizational source. It is being released in the interest of making available as much information as possible.

- This document may contain data, which exceeds the sheet parameters. It was furnished in this condition by the organizational source and is the best copy available.

- This document may contain tone-on-tone or color graphs, charts and/or pictures, which have been reproduced in black and white.

- This document is paginated as submitted by the original source.

- Portions of this document are not fully legible due to the historical nature of some of the material. However, it is the best reproduction available from the original submission.
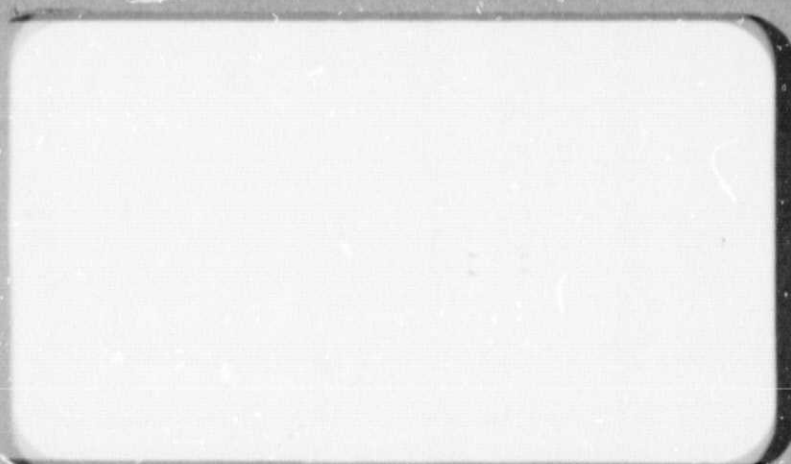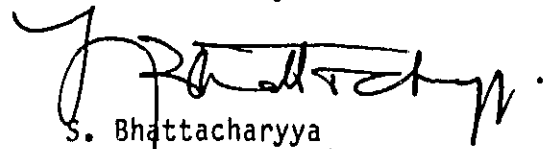
iiTRi
IIT Research Institute

FOREWORD

This is the first quarterly narrative report summarizing the work done during 7 December 1982 to 28 February 1983 on the NASA Project, "Creep-Rupture Behavior of Iron Superalloys in High-Pressure Hydrogen." This project is under NASA Contract No. DEN3-303, and the IITRI designation for this report is IITRI-M06116-3.

During this quarter, procurement and fabrication of equipment items to test four cast and two wrought alloy specimens were completed. In addition, sensitive micrometers for external monitoring of creep strain were integrated to the system. Computer programs were written to obtain the creep strain-time master curves from which time to specific strain values could be easily obtained.

Test H13 at 760°C (1400°F) for 200 h estimated rupture life was concluded, and test H14 at 760°C (1400°F) for 500 h estimated rupture life was initiated, of which 450 h of testing has been completed during the reporting period. Significant analysis of the initial data was accomplished along with fracture surface observation and analysis.

In December 1982, NASA CR-16807 "Creep-Rupture Behavior of Six Candidate Stirling Engine Iron-Base Superalloys in High Pressure Hydrogen, Volume 1 - Air Creep-Rupture Evaluation," was published as the final report under NASA Contract DEN3-217.

The following people contributed to the program: J. Mok, W. Peterman, and T. Todner. The report was typed by M. Dineen and edited by V. Johnson.
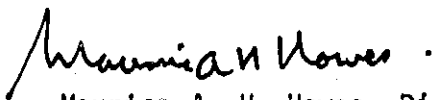
S. Bhattacharyya
Senior Metallurgist

Maurice A. H. Howes, Director
Materials Technology Division

TABLE OF CONTENTS

LIST OF TABLES

LIST OF FIGURES

IIT RESEARCH INSTITUTE

IITRI-M06116-3

1. INTRODUCTION

The objective of this program is to evaluate the creep-rupture properties of five candidate iron-base and one cobalt-base high-temperature alloys for use as construction materials in the Stirling engine. The creep-rupture properties of these alloys at 760° and 815°C (1400° and 1500°F) will be determined in 15.0 MPa (2175 psi) H_2 for 200 to 1000 h. The resulting data will be analyzed and correlated with creep-rupture data generated in Tasks I and II of Contract DEN3-217.

2. TECHNICAL PROGRESS SUMMARY

The project, initiated on 7 December 1982, consists of the following tasks:

Task I: Material Preparation for H_2 Creep-Rupture Testing

Task II: Creep-Rupture Testing in High-Pressure Hydrogen

Task III: Analysis of Data

Task IV: Reporting Requirements

This is the first quarterly narrative report covering the work performed during 7 December 1982 to 28 February 1983.

2.1 TASK I – MATERIAL PREPARATION FOR HYDROGEN CREEP-RUPTURE TESTING

2.1.1 Material Preparation

The alloys selected for testing were four cast alloys--XF-818, CRM-6D, SA-F11, and HS-31--and two wrought alloys, CG-27 and 12RN72. Investment cast alloy and sheet specimen blanks were supplied by NASA. IITRI was informed that the cast alloys were radiographed before shipment, and these as well as 12RN72 were obtained from United Stirling AB, Sweden. The CG-27 was obtained from Crucible Steel Co., USA. The nominal compositions of these six alloys are given in Table 1.

The test specimens were supplied according to Fig. 1. The as-cast speci-
mens were machined, and the gage length was ground to 3.18 mm (0.125 in.)
diameter with a 0.81 μm (32 microinch) rms surface finish. The sheet speci-
mens were received in the finish machined condition except that the pin-hole
distances were too close for testing in the existing grips. New A-286 alloy
tabs were laser-welded at both ends and new holes drilled for testing. A
photograph of typical specimens is shown in Fig. 2.

2.1.2 Heat Treatment

All the cast alloy specimens in the fully machined condition were given
an identical simulative brazing cycle heat treatment by NASA. The specimens
were heat treated in 10^{-6} mm vacuum at 1150°C (2100°F) for 1 h and furnace
cooled.

12RN72 is a Sandvik tube alloy, specially rolled into sheet form for
United Stirling AB and obtained by NASA. It is believed to have been given a
solution annealing treatment at 1150°C (2100°F) for 15 min and rapidly cooled
in air or water.

CG-27 was heat treated at 1150°C (2100°F) in vacuum for 10 min and
furnace cooled to room temperature. It is then aged at 790°C (1450°F) in
vacuum for 16 h, cooled to 650°C (1200°F), held for 24 h, and furnace cooled.

2.1.3 Hardness Measurement

Rockwell hardness measurements were made on the longitudinal half-section
of the threaded portion of the four cast alloys (heat treated) and coupons of
the two sheet alloys supplied by NASA. These values are given in Table 2.

Three of the four cast alloys have practically the same hardness with
XF-818 having a distinctly lower hardness most likely related to its low
carbon level (0.2%). Wrought alloy CG-27, because of the aging treatment,
shows a very high hardness of 367 HV (HRC 38).

2.1.4 Microstructure

All the six alloys have solid solution-strengthened austenitic structures
with varying amounts of precipitates depending on carbon, boron, and nitrogen
levels, type of processing (cast vs. wrought), and heat treatment. Typical
microstructures of the four cast alloys and the two sheet alloys are shown in
Figs. 3 and 4.

IIT RESEARCH INSTITUTE

IITRI-M06116-3

In Figs. 3a to d, at 50X, the typical dendritic structures of the cast alloys are clearly revealed. The interdendritic arm spacings are very similar, with HS31, probably showing a little coarser spacing. The grain pattern shown in Fig. 3a for XF-818 is not seen in the other cast alloys. The dendrite arms and grain boundaries usually consist of boride- and carbide-containing constituents, and the lower carbon and chromium contents of XF-818 are reflected in its lower hardness.

In Figs. 3e to h, the microstructures of the four cast alloys are shown at a higher magnification of 200X. The structures clearly indicate the discrete precipitates constituting the dendrite walls, and some coring effect is noted in CRM-6D. In HS-31, the structural continuity at the boundaries is much less in evidence and only traces of lamellar structure are noted.

Figure 4 shows the wrought alloy structures for 12RN72 and CG-27. CG-27 has more than three times the hardness (and strength) of 12RN72 at room temperature and contains Al, Ti, Cb, Ta, and Mo in quantities significantly larger than 12RN72. CG-27 alloy contains low boron and carbon. While the literature data indicate a low level of boron in 12RN72, the analysis supplied by NASA did not show that. It is possible that B at 0.006% level is present in the alloys, and this may be checked by NASA.

In the solution-treated condition (Figs. 4a and b) the 12RN72 has a fully austenitic twinned structure with some undissolved particles, identified in Sandvik literature[1] as micron-sized carbides and nitrides of type TiN.

The solution-treated and aged structure of CG-27, shown in Fig. 4c, reveals fully austenitic grains with some fine precipitates related to its Ti and Al contents. Twinning is also evident but to a much lesser degree than 12RN72. CG-27 grain size is over three times larger than 12RN72.

2.2 TASK II - CREEP RUPTURE TESTING IN HIGH-PRESSURE HYDROGEN

The present 6-test program is outlined in Table 3. The project was initiated with tests at 760°C (1400°F). The first two tests, H13 and H14,

---

[1]Sandvik Lecture No. 56-10E, FS1, March 1978.

IIT RESEARCH INSTITUTE

IITRI-M06116-3

were set for 200 and 500 h rupture lives. The initial stresses for these tests were selected by NASA based on air-creep tests at NASA laboratory, and the selected stress values are given in Table 4. In Appendix A, some details are given regarding load calculations to obtain these initial stress values. Test H13 is completed, and test H14 is expected to be over during the first week of March.

2.3 TASK III - ANALYSIS OF DATA

The results to date are summarized in Tables 5 and 6 for tests H13 and H14, respectively. To compare H13 and H14 rupture life data in 15 MPa H_2 with NASA data in air, these values are plotted on Fig. 5 where estimated lines are drawn through the NASA data for rupture life.

2.3.1 Rupture Life vs. Stress (Figure 5)

Of the four cast alloys tested in air by NASA, XF-818 and HS-31 have similar and very high stress life exponents. CRM-6D and SA-F11 have almost identical slopes which are about one-half those for XF-818 and HS-31. The two wrought alloys have similar slopes and almost equal to those of cast alloys CRM-6D and SA-F11.

The IITRI data (solid symbols) indicate that 15 MPa H_2 does not seem to affect rupture life in XF-818 and CRM-6D with a possibly marginal lowering in HS-31. Enough data are not available for SA-F11, 12RN72, and CG-27 to draw even tentative conclusions. More detailed analysis will be performed when more results become available at the end of the next quarter.

2.3.2 Creep Strain-Time Plots

Capacitance-type transducers from inside the high pressure chamber send signals which are kept in floppy disks, printed on charts, and displayed on a TV screen. The transducers indicate values to the nearest 0.25 µm (10 µin.). Once in a while these sensitive transducers were observed to get stuck internally indicating a lower reading. As a cross-check, dial micrometers, reading to the nearest 5 µm (200 µin.) were mounted on each arm where a lever ratio magnification of actual specimen extension by a factor of about 8 will be obtained. These results, as shown in Appendix B, indicate both the internally and externally measured extension data to be highly reproducible.

The data in the floppy disk were decoded and converted to graphical time-creep strain plots using a specially written computer program. Typical creep strain-time plots for a few alloys are shown in Figs. 6 to 14.

With the help of scale magnification, it is possible to obtain the time-strain plots to reveal details which will be difficult to obtain otherwise. Generally, after the first 1 or 1-1/2 h, the data collection is done every 4 h and, for test durations of 200 to 1000 h, a frequency of 4 h reveals the information within the desirable accuracy. A comparison of different scale magnifications through computer is shown for HS-31 data from test H14 in Figs. 15, 16, and 17. From Fig. 15, one can obtain the specific times to 0.1, 0.2, 0.5, 1.0, and 2.0% creep strains; Figs. 16 and 17 both permit a measure of the minimum creep rate, while Fig. 17 permits an accurate measure of the time to onset of tertiary creep. The plateau in Fig. 17 indicates the limiting range of the transducer where it got stuck and then jumped to a higher value on fracture. A careful examination of all the figures indicates that a fracture event has no effect on the creep behavior of the rest of the specimens (compare Figs. 6, 8, 10, and 12 for test H13, and Figs. 7, 9, 11, 13, and 14 for test H14).

2.3.3 Macroscopic Observation of Fracture

The four cast specimen fractures were evaluated for their appearance and localized reduction in area. The reduction in area values correlate well with the total elongation value as shown in Table 7. The total elongation values, the reduction in areas, and the last extension (and time) before rupture are given in Table 7 for test H13.

CRM-6D, because of high stress and short rupture life, exhibited a significant ductility of 20.1% elongation and 35.0% reduction in area. Shortly before rupture, at 3.3 h (t_r = 3.7 h), the observed creep extension was 11.9% (Fig. 8). It is obvious that significant elongation took place on fracturing to give a total elongation of 20.1%. Fracture observations on all four cast alloys are summarized in Table 8.

HS-31 showed a very high total elongation of 23.2%. Nine hours before failure, at 184 h (t_r - 193 h), creep extension was 18.1% and, again, a significant ductile elongation took place on fracture as described in Table 8.

XF-818 ductility on fracture was less than those of HS-31 and CRM-6D. It showed less ductility at fracture when recorded at 254 h, 4 h before rupture at 258 h. The entire specimen surface showed uneven deformation due to metal flow as described in Table 8.

SA-F11 had the least ductility of the four cast alloys and showed no additional ductility at rupture. When the measurement was made 2 h before $t_r = 336$, the creep strain was comparable with total elongation. The fracture was off-center near the edge of the gage length, as described in Table 8.

2.4 TASK IV - REPORT REQUIREMENTS

Monthly reports of December 1982 and January 1983 were submitted on time.

3. PROBLEM AREAS

The sheet specimens supplied were 9.53 mm (0.375 in.) wide, whereas in all prior tests sheet specimen width was kept at 6.35 mm (0.250 in.). Also, CG-27, a very strong alloy, was significantly thicker than 12RN72; CG-27 had a thickness of about 1 mm (0.039 in.). During testing in the first two tests, it was realized that CG-27 with its combination of higher thickness and wider gage section was requiring the use of a very large total load approaching 2.67 kN (600 lbf). A large load requires a thicker pullwire which had to be bent over a small radius, creating weakness and a potential for pullwire rupture inside the pressure vessel. It had happened once during the first 12 tests under DEN3-217. In test H14, described earlier, the CG-27 pullwire broke on full loading. For future tests, starting with H15, the remaining CG-27 specimens have been machined to a uniform width of 6.35 mm (0.250 in.) for which the equipment was designed. This will allow use of thinner pullwires with less damage during small radius looping and consequent failure possibilities.

Pullwires currently in use are 302 stainless steel spring wire. The two sizes used most frequently are 2.03 mm (0.080 in.) and 1.60 mm (0.063 in.) diameter. Typical ultimate strength values of these pullwires are given below:[*]

Wire Diameter, mm (in.)		Area, mm^2 (10^{-3} $in.^2$)		UTS, GPa (ksi)		Breaking Load, kN (lbf)	
1.04	(0.041)	0.85	(1.32)	1.88	(272)	1.60	(359)
1.60	(0.063)	2.01	(3.12)	1.74	(252)	3.49	(785)
2.03	(0.080)	3.24	(5.03)	1.67	(242)	5.41	(1216)
2.41	(0.095)	4.56	(7.09)	1.60	(232)	7.30	(1640)

---

[*]ASM Metals Handbook, 9th Edition, Vol. 3, p. 14, American Society for Metals, Metals Park, Ohio.

Contract No. DEN3-303
Report No. IITRI-M06116-3

CREEP-RUPTURE BEHAVIOR OF IRON SUPERALLOYS
IN HIGH-PRESSURE HYDROGEN

NASA-Lewis Research Center
21000 Brookpark Road
Cleveland, Ohio 44135

Attention: Mr. Robert Titran
             Project Manager
             Mail Stop 49-1
             Strategic Materials Section
             Materials Division

Prepared by

S. Bhattacharyya and W. Peterman

IIT Research Institute
10 West 35 Street
Chicago, Illinois 60616

14 March 1983

First Quarterly Narrative Report
for Period Covering 7 December 1982 to 28 February 1983

4. FUTURE WORK

With the completion of test H14 by March 7 to 10, test H15 will be started. It was decided by the NASA Project Monitor that H15 will be for 200 h at 815°C (1500°F). This is expected to be followed by test H16 for 500 h at 815°C (1500°F). Tests H15 and H16, with normal turnaround time, will be completed by end-April. Tests H13 and H14 have completed over 1050 h out of projected 3400 h test time.

TABLE 1. SUPERALLOY COMPOSITIONS (NOMINAL)

Element	Alloy Composition, wt%					
	CG-27	12RN72	SA-F11	XF-818	CRM-6D	HS-31[a]
Al	1.5	-	-	-	-	-
B	0.01	-	0.4	0.6	0.003	-
C	0.05	0.1	0.63	0.2	1.05	0.5
Cb+Ta	0.6	-	-	0.4	1.0	-
Co	-	-	-	-	-	54
Cr	13.0	19.0	23.0	18.0	22.0	25.5
Fe	38.0	47.0	47.0	55.0	63.0	-
Mn	0.1	1.8	0.5	0.1	5.0	0.75
Mo	5.5	1.4	-	7.5	1.0	-
N	-	0.015	-	-	-	-
Ni	38.0	30.0	16.0	18.0	5.0	10.5
Si	0.1	0.29	0.6	0.3	0.50	0.75
Ti	2.5	0.5	-	-	-	-
W	-	-	12.0	-	1.0	7.5

[a]ASM Metals Handbook, Vol. 3, 9th Ed., p. 268; other compositions indicated by NASA.

TABLE 2. HARDNESS OF SIX SUPERALLOYS

Alloy	Hardness, HRA	Average Hardness HRA (HV)[a]	
XF-818	48.5, 53.8, 54.0	52.1	(164)
CRM-6D	60.7, 60.5, 63.6	61.6	(249)
HS-31	59.0, 62.0, 62.0	61.0	(243)
SA-F11	60.0, 62.0, 62.0, 61.2	62.1	(256)
12RN72	38.5, 40.5, 40.2	39.7	(107)
CG-27	70.0, 70.0, 69.0	69.7	(378)
	Rockwell Superficial Scales[b]		
12RN72	57.5, 57.3, 55.0 (30T)	56.5 (HR 30T)	(107) (HV)
CG-27	56.8, 57.4, 57.4 (30N)	57.2 (HR 30N)	(367) (HV)

[a]Standard Hardness Conversion Table for Metals, ASTM Std. E140-79, 1982 Annual Books of ASTM Standards, Part 10, p. 359.

[b]12RN72 and CG-27 were also measured in Rockwell superficial scales.

TABLE 3.   CREEP-RUPTURE TEST MATRIX FOR EACH ALLOY

Atmosphere	Test Temperature		Rupture Life (approximate), h		
	°C	°F	200	500	1000
15 MPa H$_2$ (2175 psi)	760	1400	H13	H14	X
	815	1500	X	X	X

TABLE 4.   NASA-SELECTED INITIAL STRESSES FOR TESTS H13 AND H14, 760°C, 15 MPa H$_2$

Alloy	Selected Initial Stress for Rupture, MPa (ksi)	
	In 200 h (H13)	In 500 h (H14)
XF-818	195 (28.3)	185 (26.8)
CRM-6D	255 (37.0)	130 (18.9)
HS-31	245 (25.5)	235 (34.1)
SA-F11	260 (37.7)	230 (33.4)
12RN72	100 (14.5)	90 (13.1)
CG-27	200 (29.0)	265 (38.4)

TABLE 5. TEST H13, CREEP-RUPTURE TEST AT 760°C IN 15 MPa H_2

Alloy	Stress, MPa	Rupture Life (t_r) h	Minimum Creep Rate ($\dot{\varepsilon}_m$) s^{-1}	Time to 1% Creep Strain, h	Time to Tertiary Stage, h	Total Elong., %	Red. in Area, %
XF-818	195	258	6.32E-08	35.0	55.0	11.6	20.7
CRM-6D	255	3.7	5.21E-06	0.4	1.0	20.1	35.0
HS-31	245	193	2.04E-07	3.0	125	23.2	42.6
SA-F11	260	336	2.33E-08	62.0	150	6.1	8.4
12RN72	100	450[a]	3.20E-09	7.0	350	3.8	-
CG-27	200	450[a]	1.10E-08	5.0	325	4.4	-

[a]Test discontinued without specimen rupture.

TABLE 6. TEST H14, CREEP-RUPTURE TEST AT 760°C IN 15 MPa H_2

Alloy	Stress, MPa	Rupture Life (t_r) h	Minimun Creep Rate ($\dot{\varepsilon}_m$) s^{-1}	Time to 1% Creep Strain, h	Time to Tertiary Stage, h	Total Elong., %
XF-818	185	325	5.72E-08	36.0	100	13.1[a]
CRM-6D	130	357	6.54E-08	27.0	150	13.5[a]
HS-31	235	245	1.73E-07	2.6	165	15.2[a]
SA-F11	230	445[b]	1.11E-08	113	210	2.7[c]
12RN72	90	247	1.14E-07	32.5	195	9.3[a]
CG-27	265	d	-	-	-	-

[a]Measured extension before rupture; after test elongation will be larger.

[b]Test continuing.

[c]Continuing test, extension at 447 h.

[d]Specimen pullwire linkage broke on full loading.

## TABLE 7. TOTAL ELONGATION, REDUCTION IN AREA, AND OTHER STRAIN DATA FOR TEST H13

Alloy	Rupture Life, h	Total Elong., %	Reduction in Area, %	Last Measured Creep Strain and Time Before Rupture	
				Strain, %	Time, h
XF-818	258	11.6	20.7	9.6	254
CRM-6D	3.7	20.1	35.0	11.9	3.3
HS-31	193	23.2	42.6	18.1	184
SA-F11	336	6.1	8.4	6.1	334
12RN72	450[a]	3.8	-	b	-
CG-27	450[a]	4.4	-	b	- .

[a]Test terminated without failure.

[b]Transducer malfunctioned.

TABLE 8. FRACTOGRAPHIC ANALYSIS OF TEST H13 SPECIMENS
Observations Made with 30X Stereomicroscope

### XF-818. Reduction in Area - 20.7%
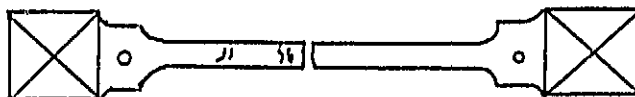
The fracture is centrally located with a mixture of dull and shiny sur-faces. Shear-type lips appear near specimen surface. Only limited surface cracking beyond rupture location. On one half, a crack has opened up on the cylindrical surface about 2 mm and another at about 10 mm from the rupture area. Near the fracture surface, the cylindrical surface appears to be roughened by significant uneven deformation.

CRM-6D. Reduction in Area - 35.0%
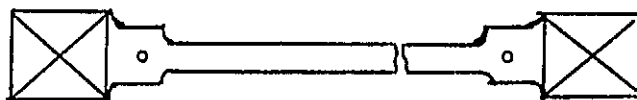
Fracture is somewhat off-center but well within the gage length. The fracture surface on the shorter piece is gray and granular with conical cen-tral prominences. The fracture surface on the longer piece has a similar cup shape indicative of ductile elongation. No significant secondary cracks on lateral surface. The dendrites are visible on the surface. Similarly to XF-818, but much more so, the entire cylinder surface extending from the fracture edge is uneven due to gross metal flow.

HS-31. Reduction in Area - 42.6%
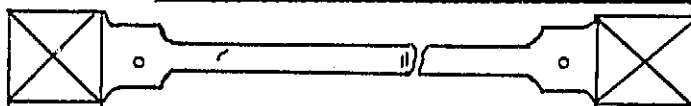
The fracture is slightly off-center. The shorter piece fracture surface shows a very significant shear mode of fracture. Remnant of dendritic pattern visible on the surface. Significant unevenness over the entire cylindrical surface of the shorter piece and also localized large diametral reduction and crack visible at 7 to 8 mm from fracture area. Some cracks are also close to the fracture. Extensive deformation and one crack about 15 mm from the frac-ture area on the longer piece.

SA-F1. Reduction in Area - 8.4%
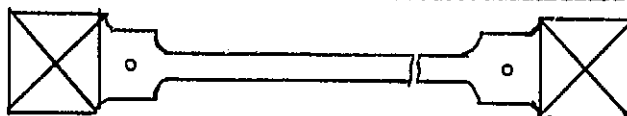
Fracture way off-center but still within the gage length. Dendrites clearly visible on the fracture surface of both the pieces. No localized cracking near or away from the fracture area. Unevenness caused by plastic deformation not evident. Both the fracture surfaces are flat without cup and cone formation, and shear lip is absent indicating lower ductility.

IITRI-M06116-3

Neg. No. 54966   50X
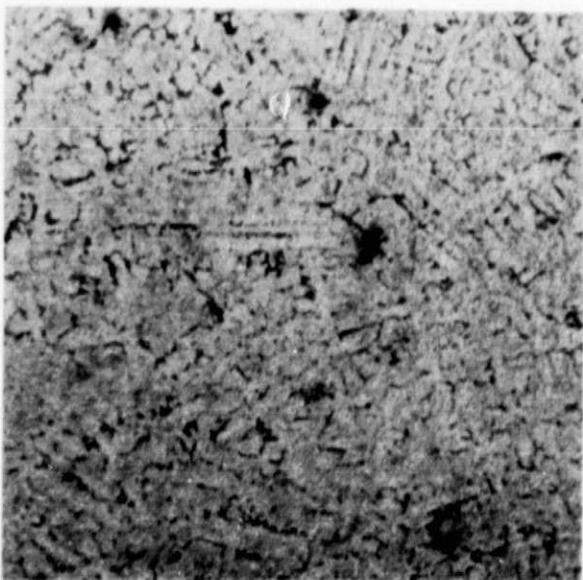
(a)

Neg. No. 45968   50X

(b)

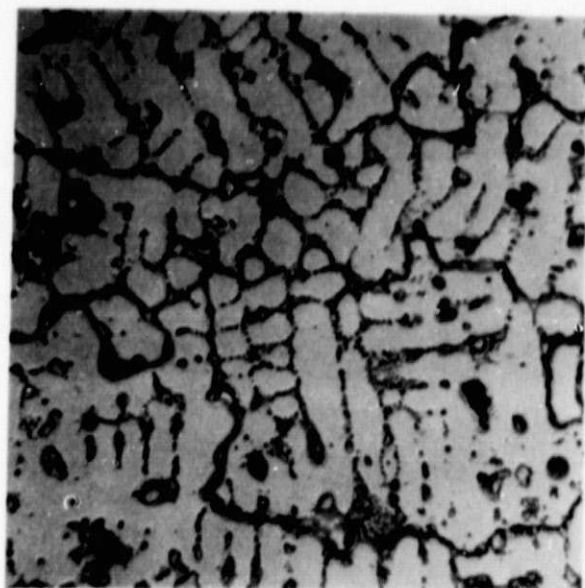Neg. No. 54961   50X

(c)

Neg. No. 54970   50X

(d)

Figure 3. Microstructure of cast alloys heat treated in 10^{-6} mm vacuum at 1150°C (2100°F) for 1 h and furnace cooled. (a,e) XF-818, (b,f) CRM-6D, (c,g) HS-31, (d,h) SA-F11. Electrolytically etched in 10% oxalic acid.
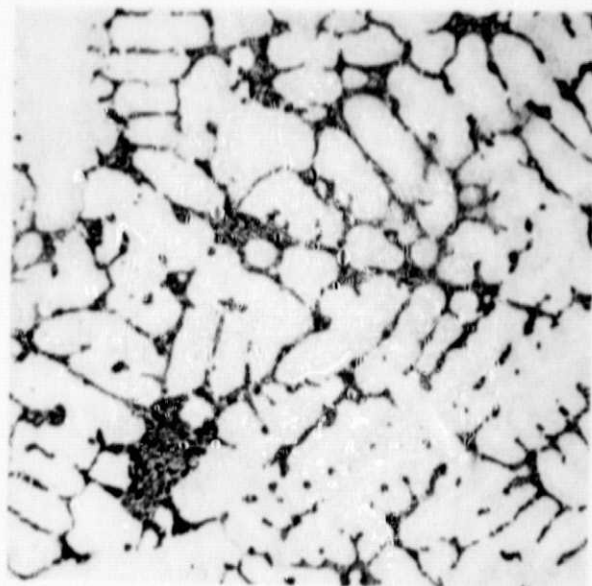
16   IITRI-M06116-3

Neg. No. 54967   200X
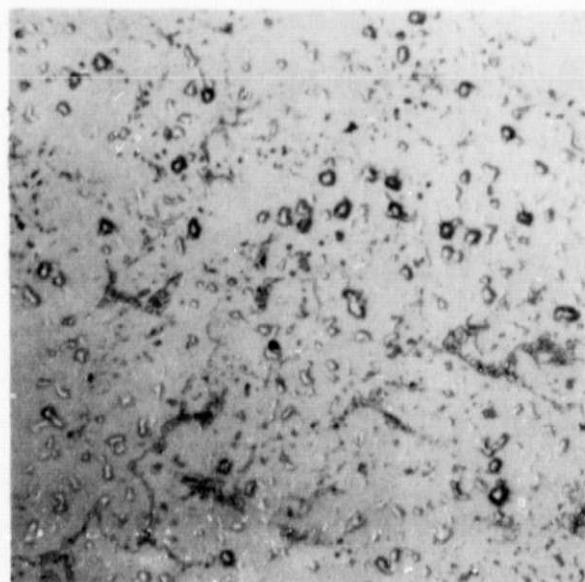
(e)

Neg. No. 54969   200X

(f)

Neg. No. 54962   200X

(g)
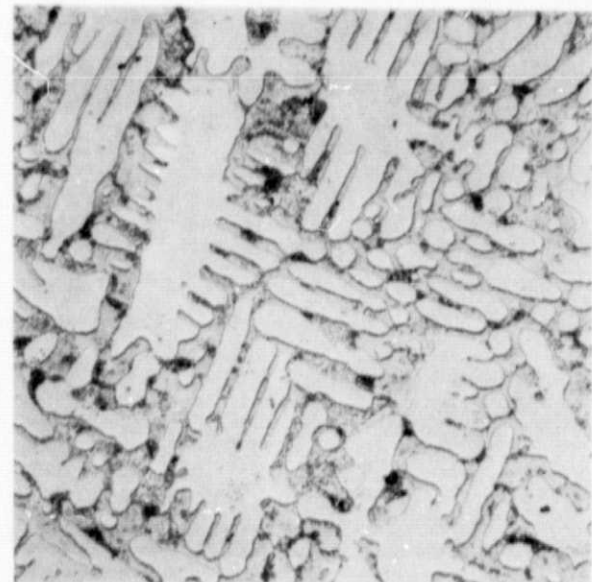
Neg. No. 54971   200X

(h)

Figure 3 (cont.)

17   IITRI-M06116-3

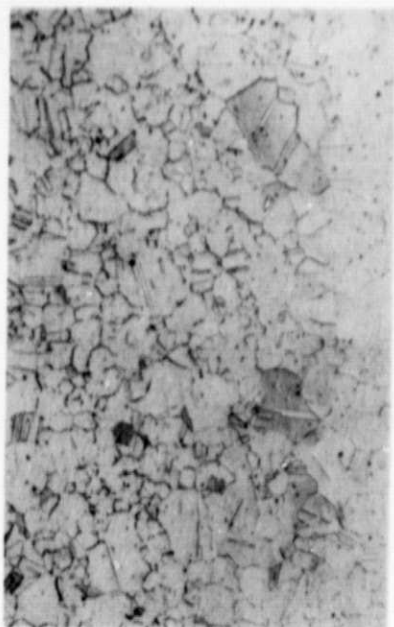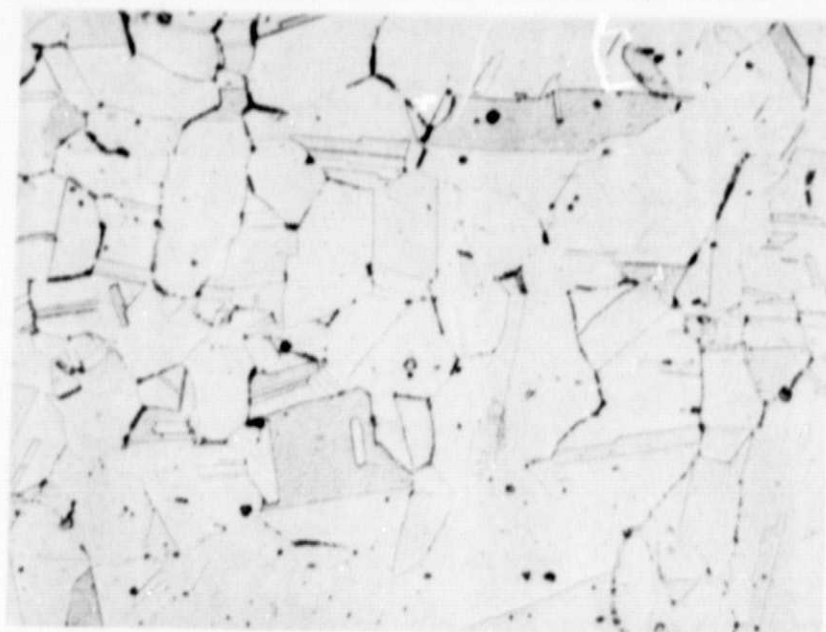Neg. No. 54963   50X   Neg. No. 54964   200X

(a)   (b)
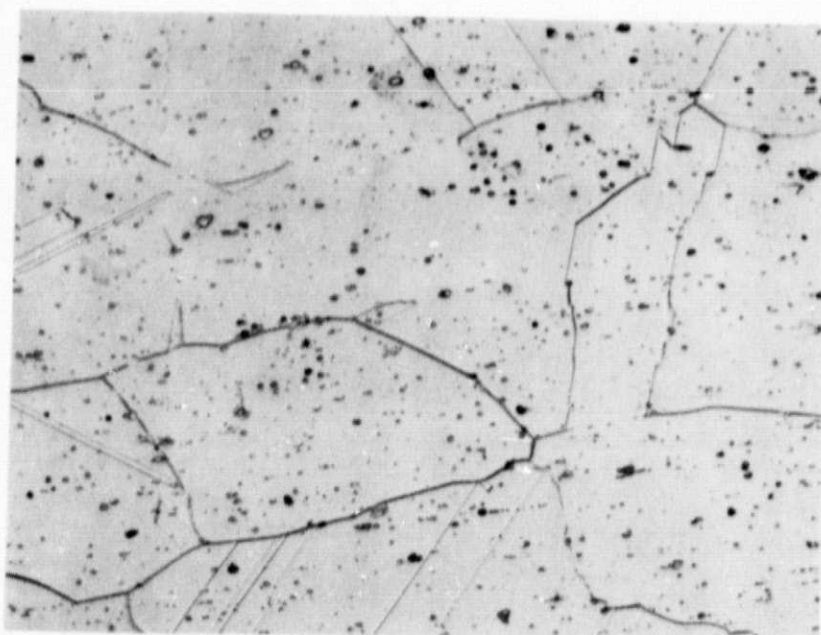
Neg. No. 54965   200X

(c)

Figure 4. Microstructure of wrought alloys. (a,b) 12RN72, solution-annealed
at 1150°C (2100°F) for 15 min and fast cooled; (c) CG-27, solution-annealed
at 1150°C (2100°F) in 10^{-6} mm vacuum for 16 h, cooled to 650°C (1200°F),
held for 24 h and furnace cooled. Electrolytically etched in 10% oxalic
acid.

18

IITRI-M06116-3

Figure 5. Rupture life vs. stress for six superalloys.

19
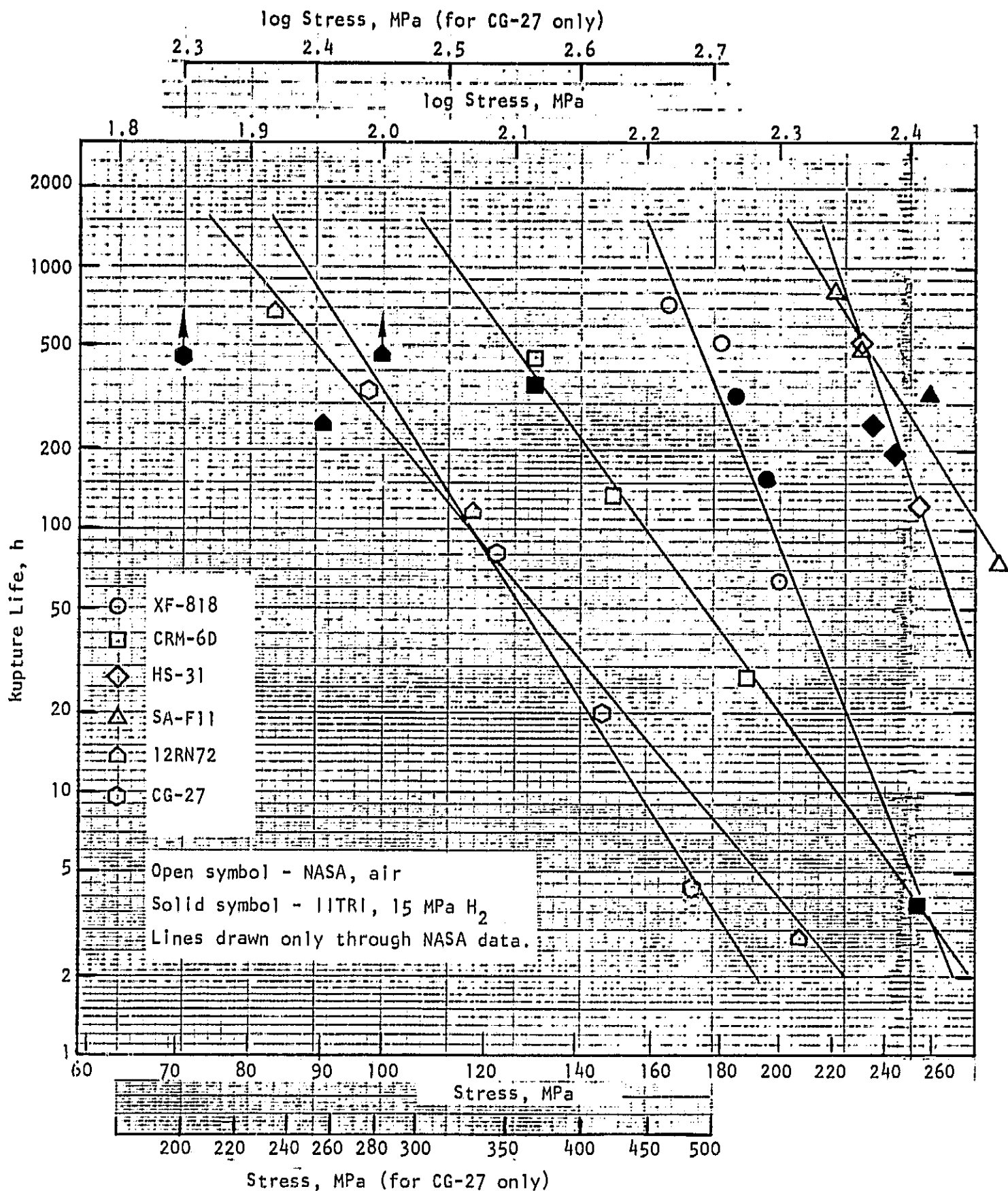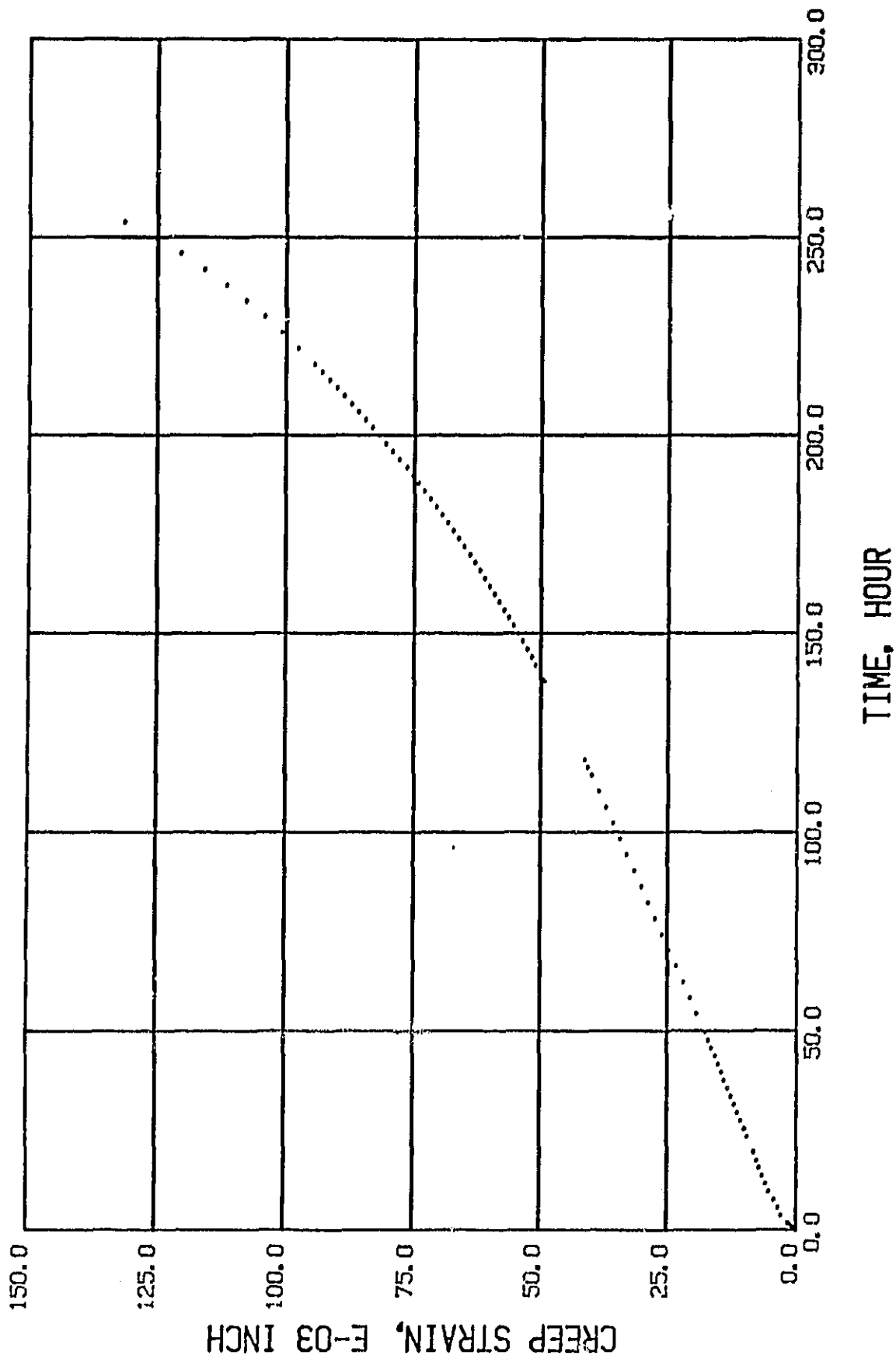
Figure 6. Creep strain-time curve for XF-818 tested at 760°C in 15 MPa H_2 (rupture life, 258 h).

IITRI-M06116-3
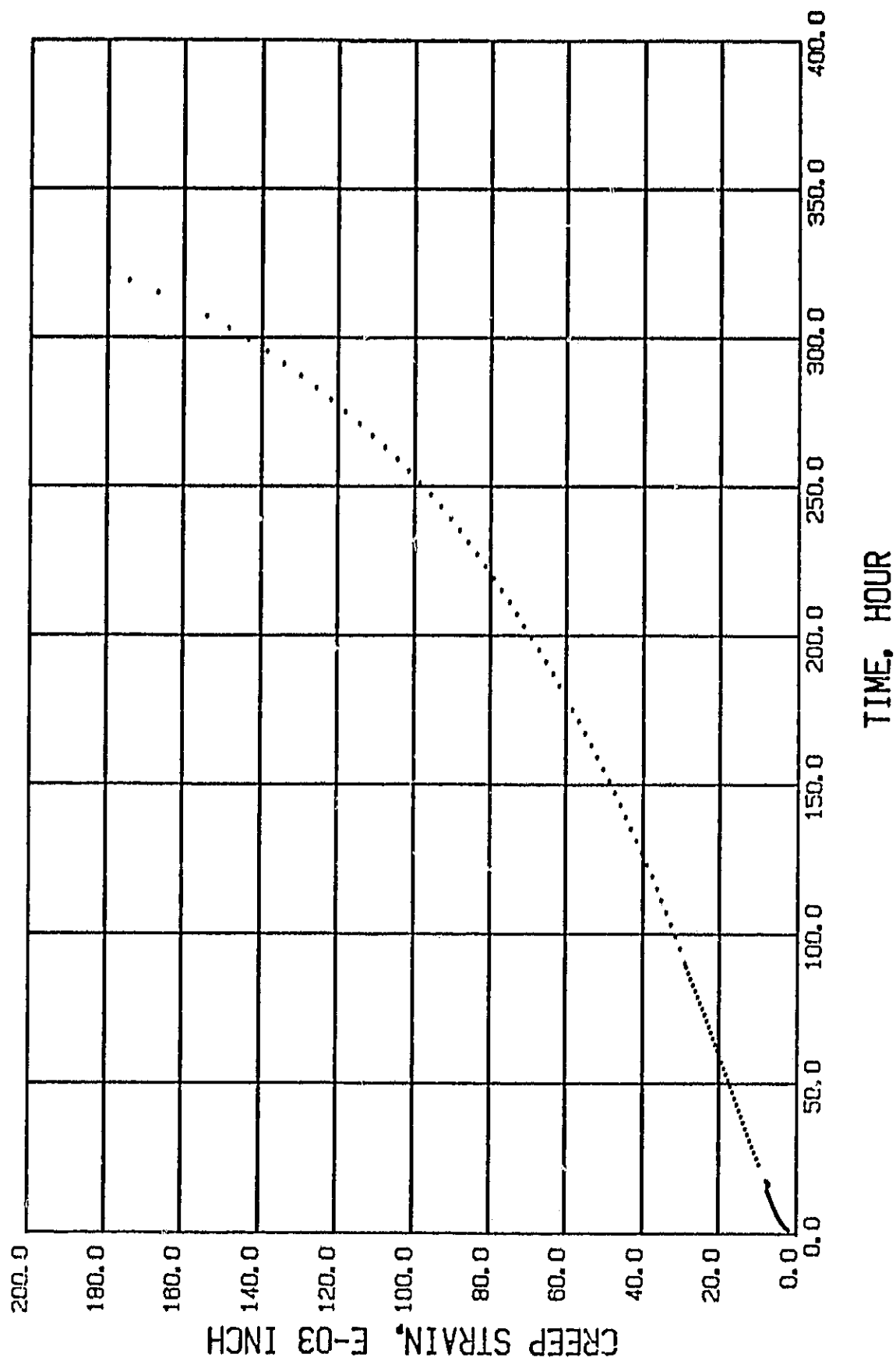
Figure 7. Creep strain-time curve for XF-818 tested at 760°C in 15 MPa H_2 (rupture life, 325 h).

IITRI-M06116-3
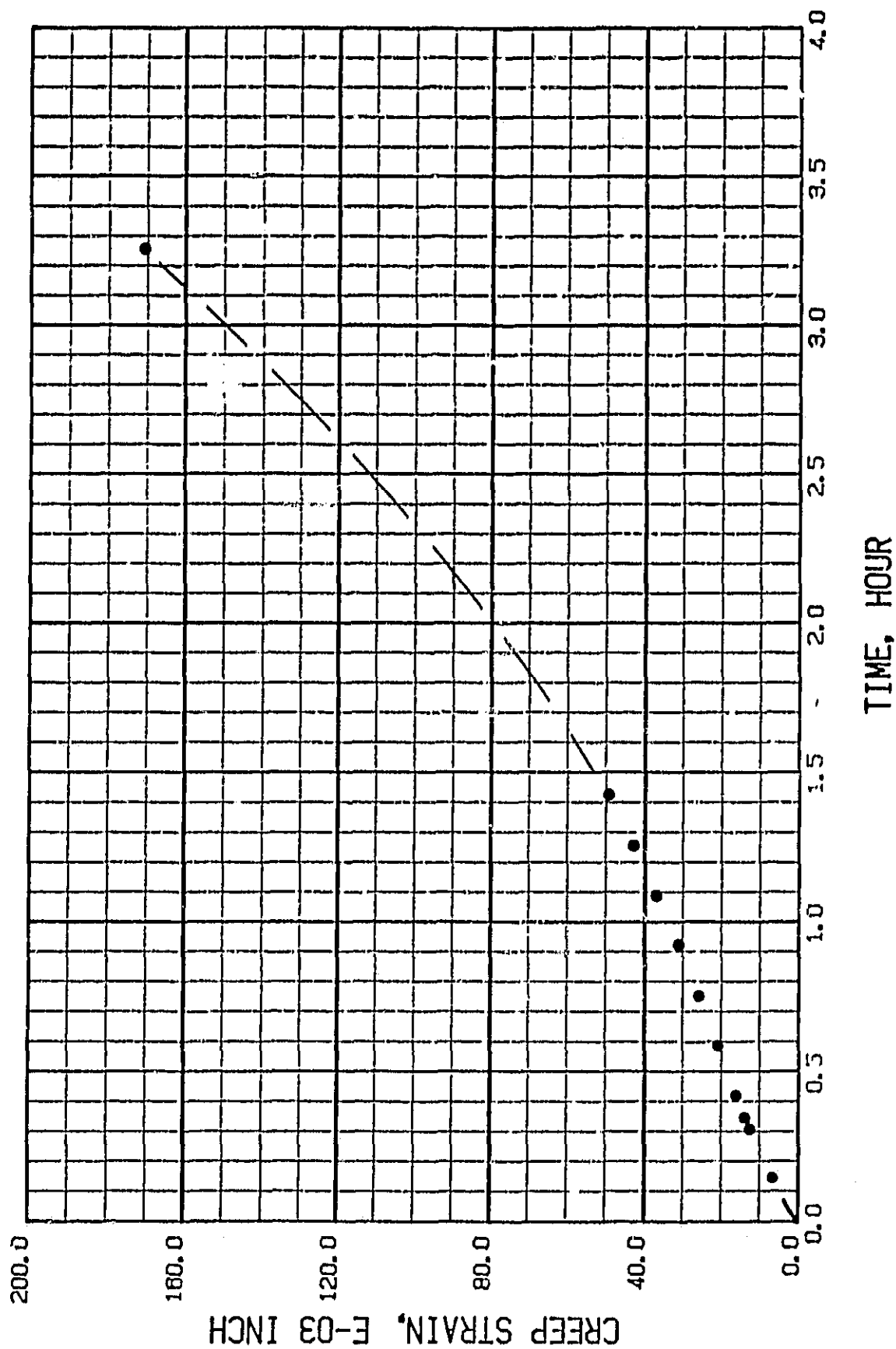
Figure 8. Creep strain-time curve for CRM-6D tested at 760°C in 15 MPa H_2 (rupture life, 3.7 h). Missing portion of data shown with a dashed curve.

22
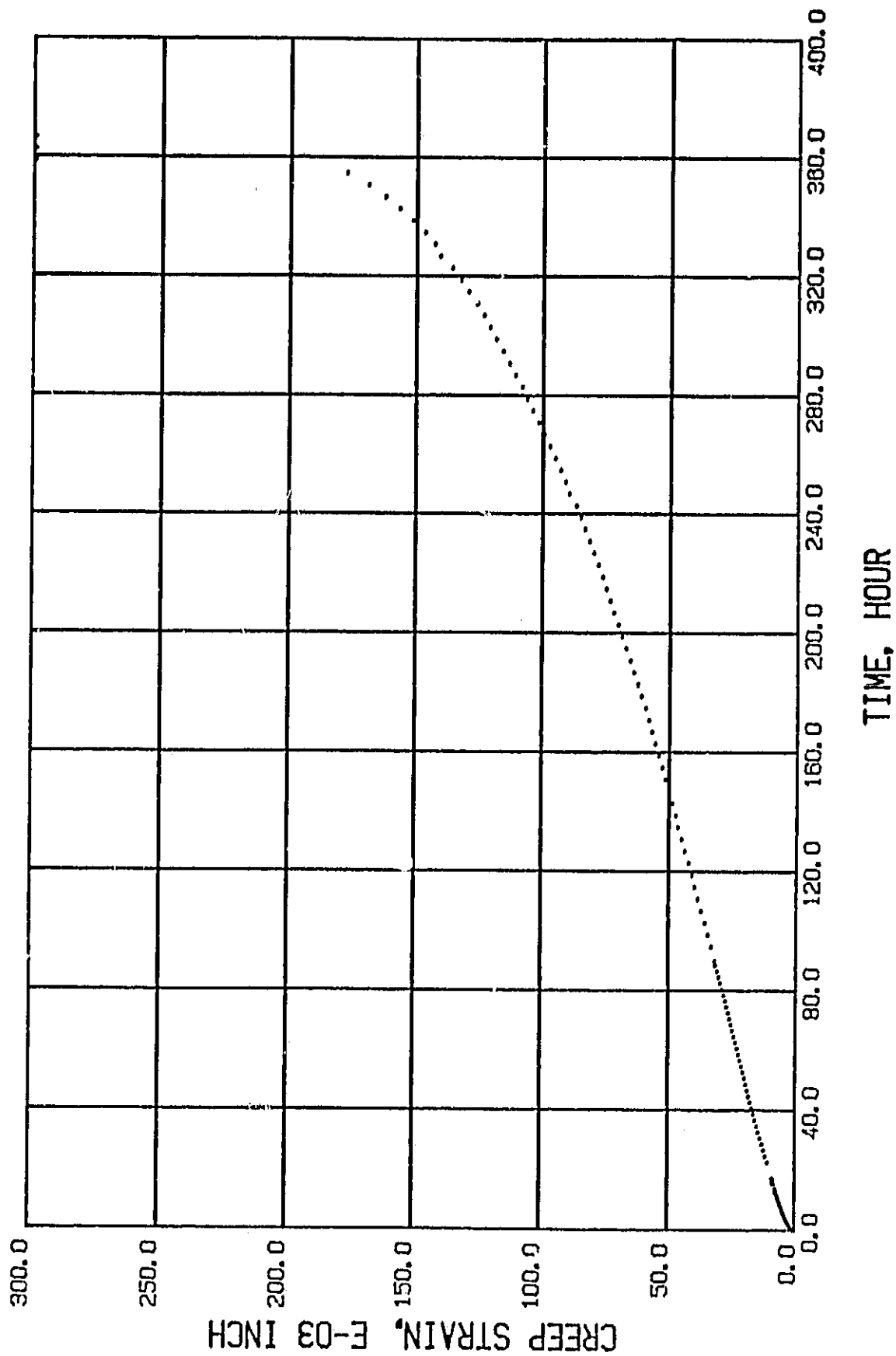
Figure 9. Creep strain-time curve for CRM-6D tested at 760°C in 15 MPa H_2 (rupture life, 357 h).

IITRI-M06116-3
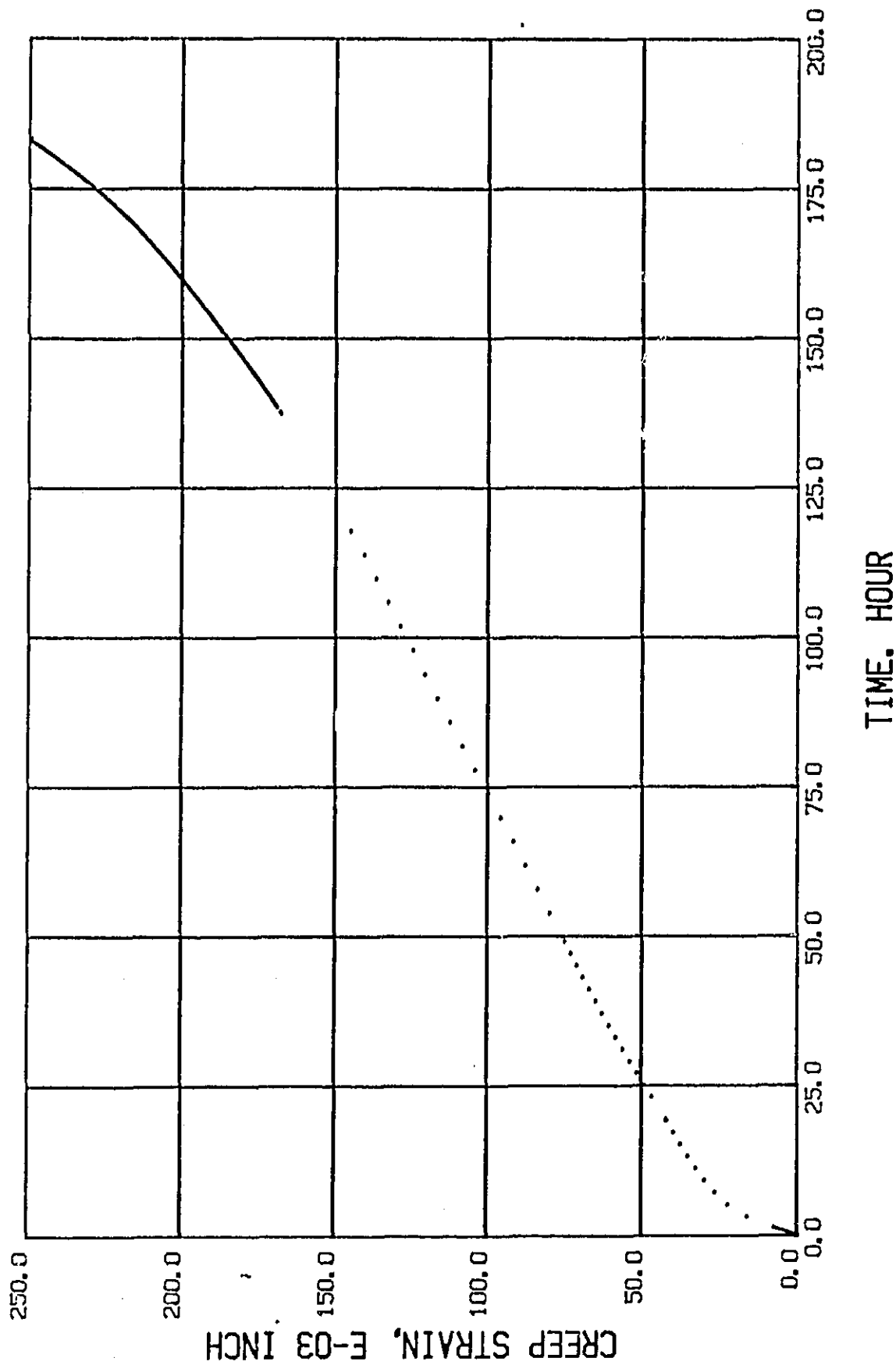
Figure 10. Creep strain-time curve for HS-31 tested at 760°C in 15 MPa H_2 (rupture life, 193 h).

IITRI-M06116-3

TEST H14   HS-31   760C./235MPa   15MPa H2

CREEP STRAIN, E-03 INCH

TIME, HOUR
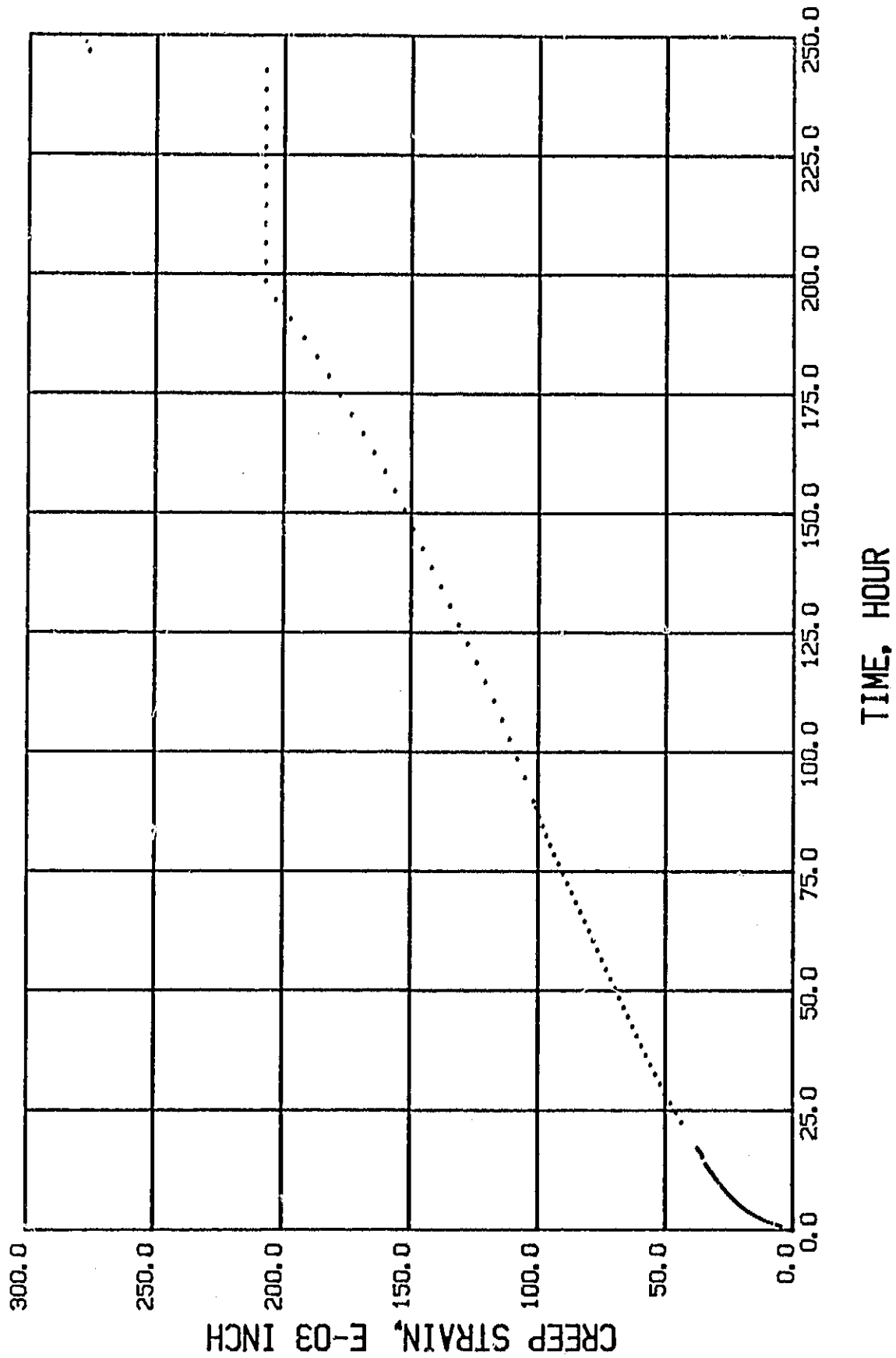
Figure 11.   *Creep strain-time curve for HS-31 tested at 760°C in 15·MPa H$_2$ (rupture life, 245 h).*

25

IITRI-M06116-3
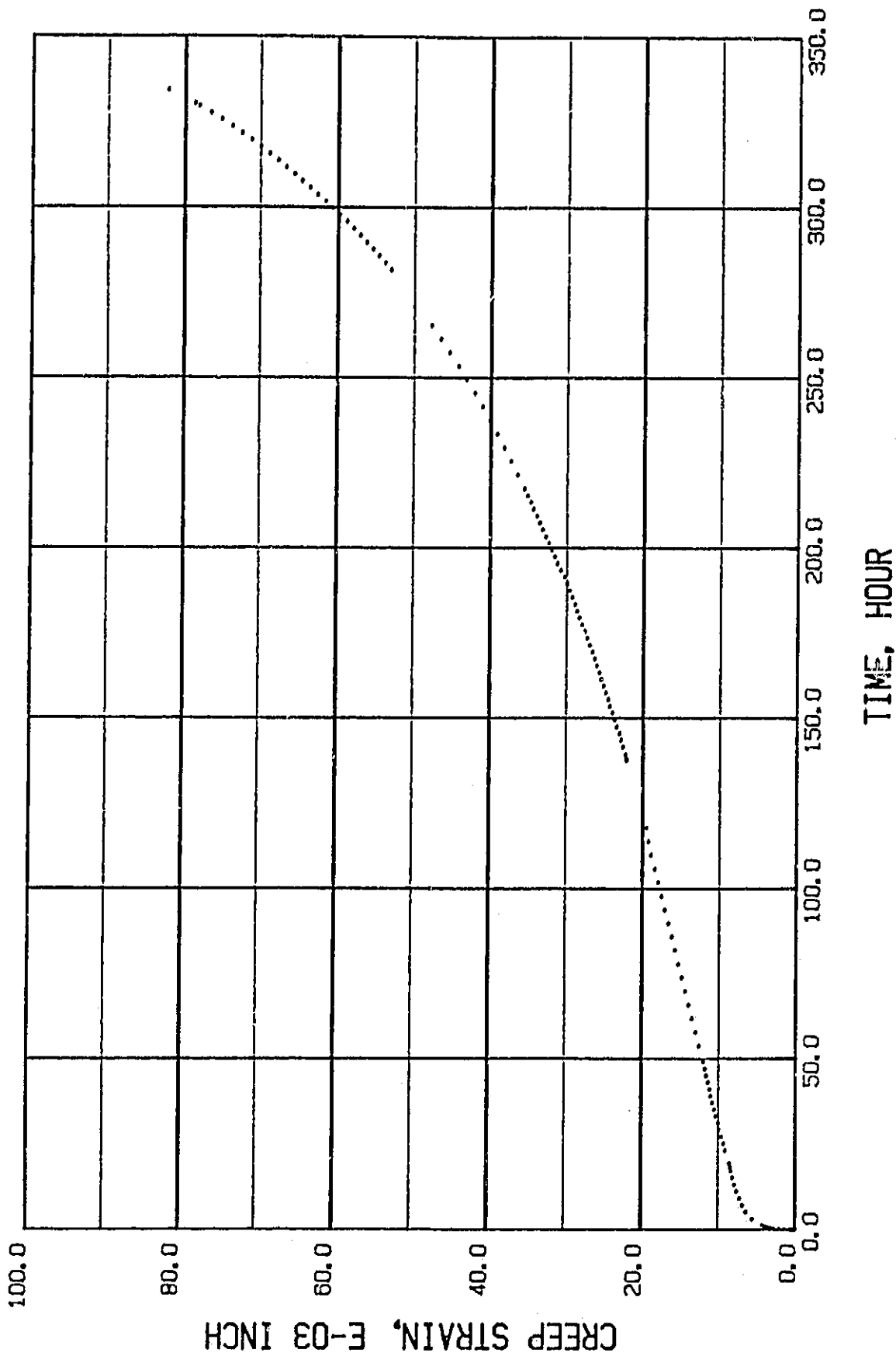
Figure 12. Creep strain-time curve for SA-F11 tested at 760°C in 15 MPa H_2 (rupture life, 336 h).

IITRI-M06116-3
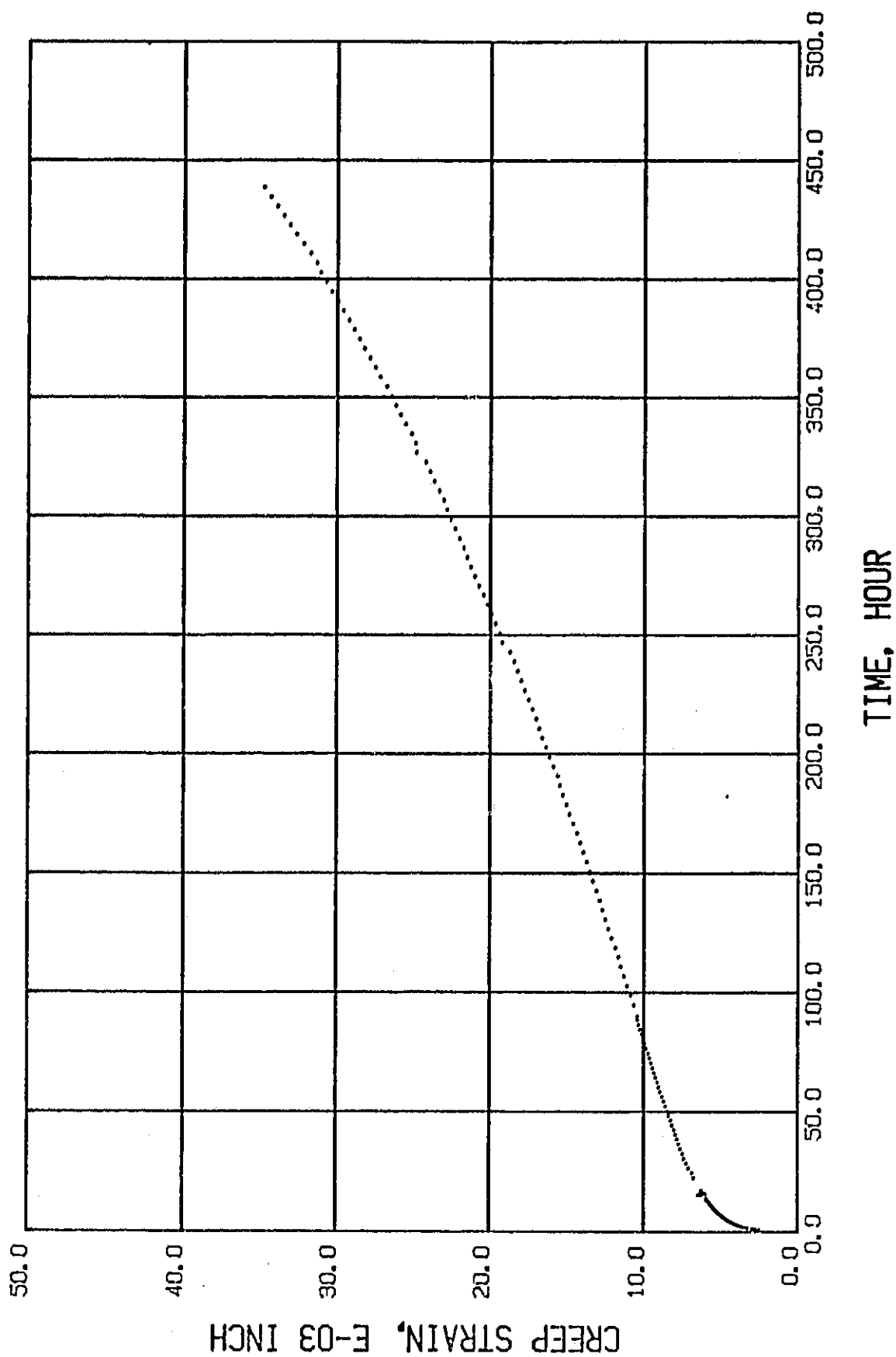
Figure 13. Creep strain-time curve for SA-F11 tested at 760°C in 15 MPa H_2 (test continuing beyond 445 h).

27
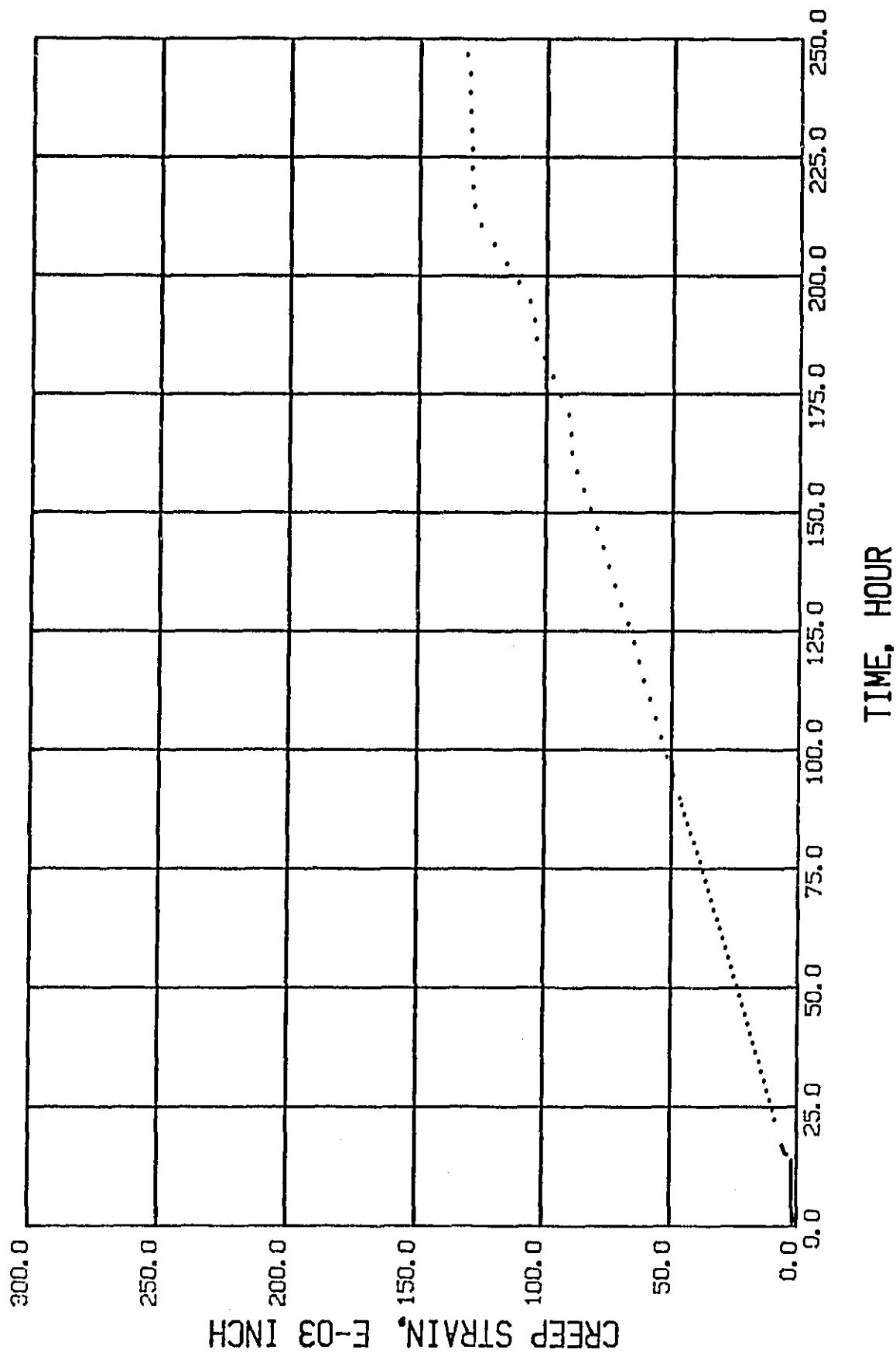
Figure 14. Creep strain-time curve for 12RN72 tested at 760°C in 15 MPa H_2 (rupture life, 247 h).

IITRI-M06116-3

TEST H14 HS-31 760C./235MPa 15MPa H2
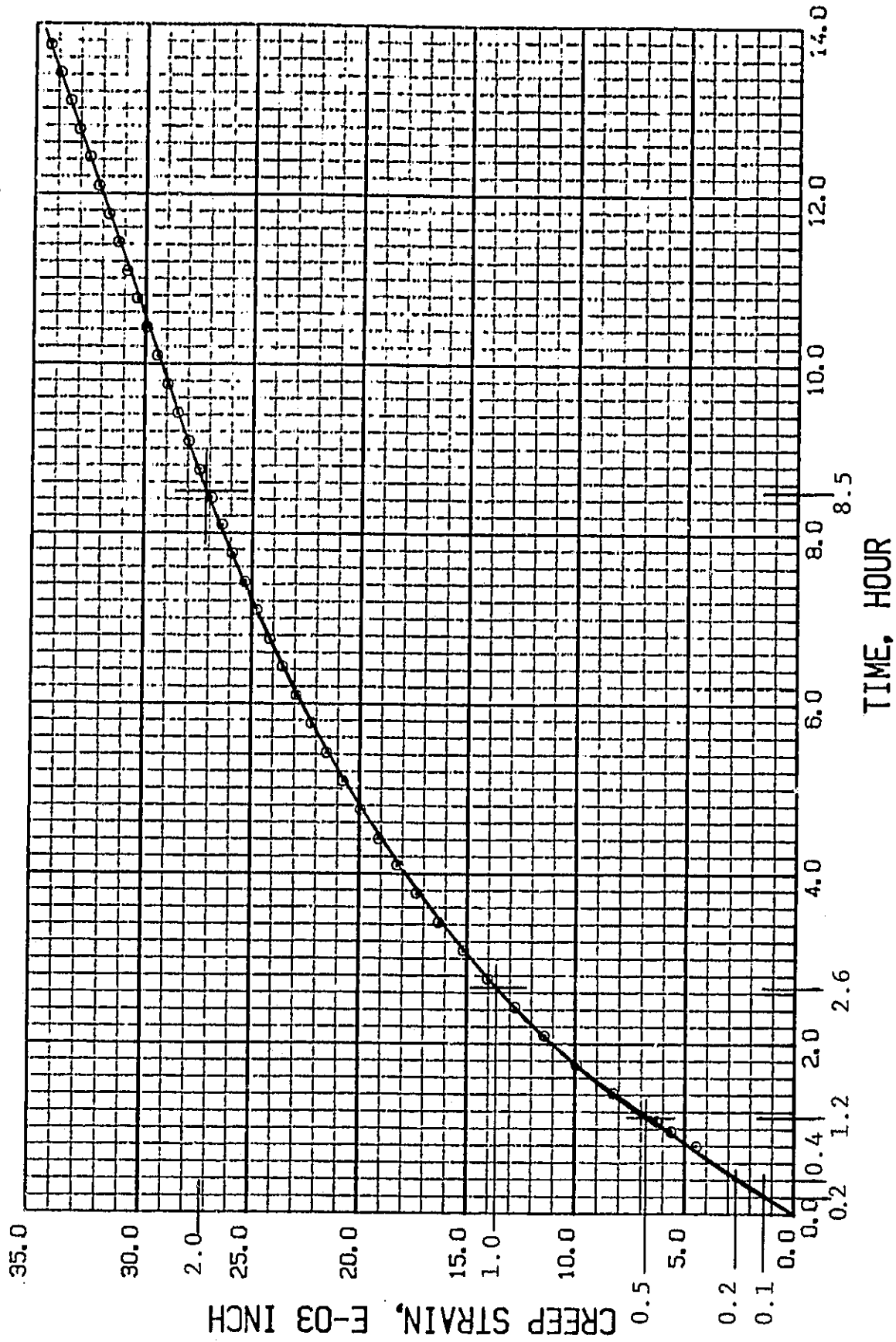
Figure 15. Creep strain-time curve for HS-31 tested at 760°C in 15 MPa H_2. Early part of the curve is shown for the evaluation of time (in hours) to reach specific creep elongations (in %).

29

IITRI-M06116-3
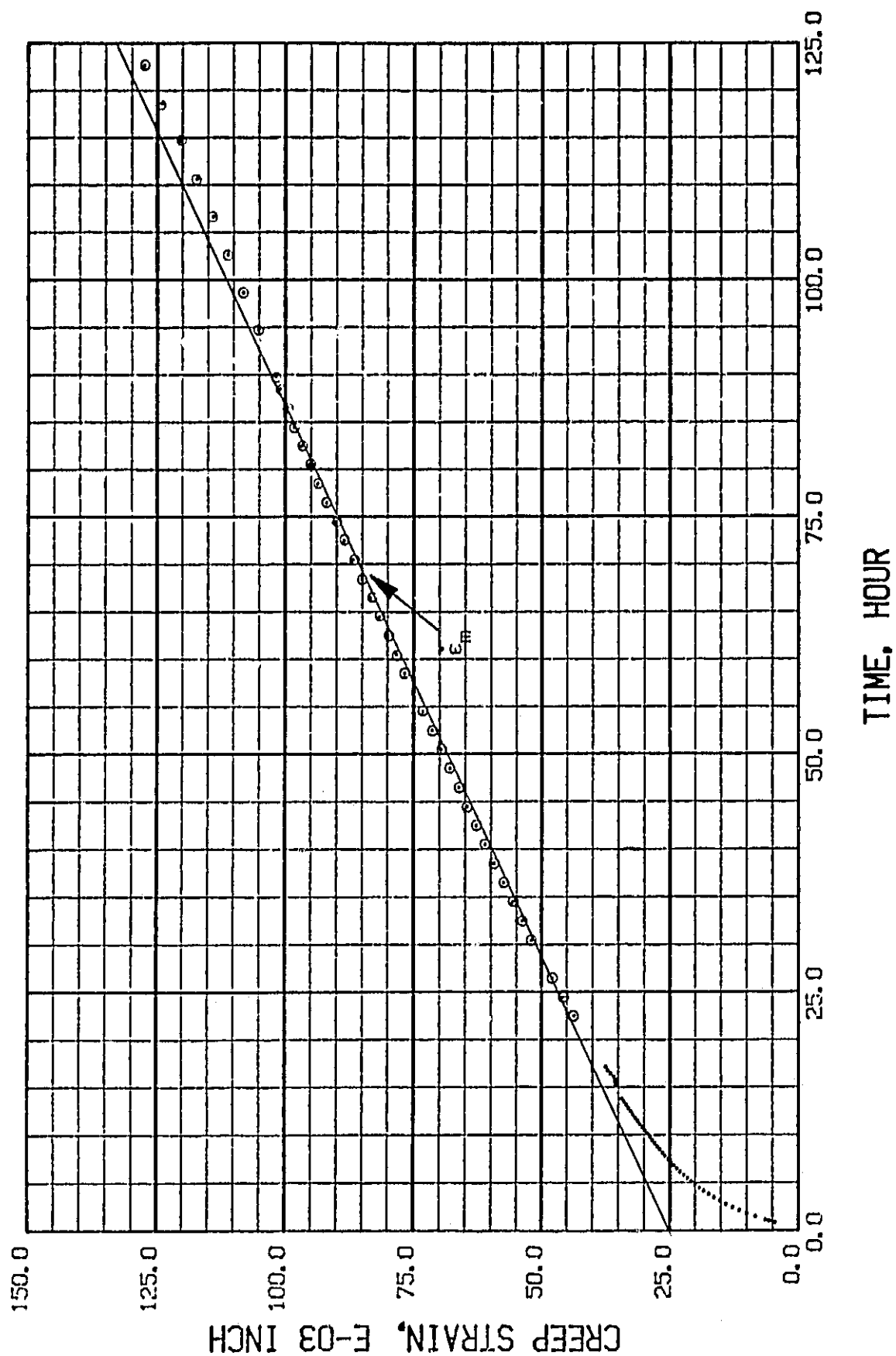
Figure 16. Creep strain-time curve for HS-31 tested at 760°C in 15 MPa H_2. Intermediate range plot to determine the minimum creep rate.

IITRI-M06116-3
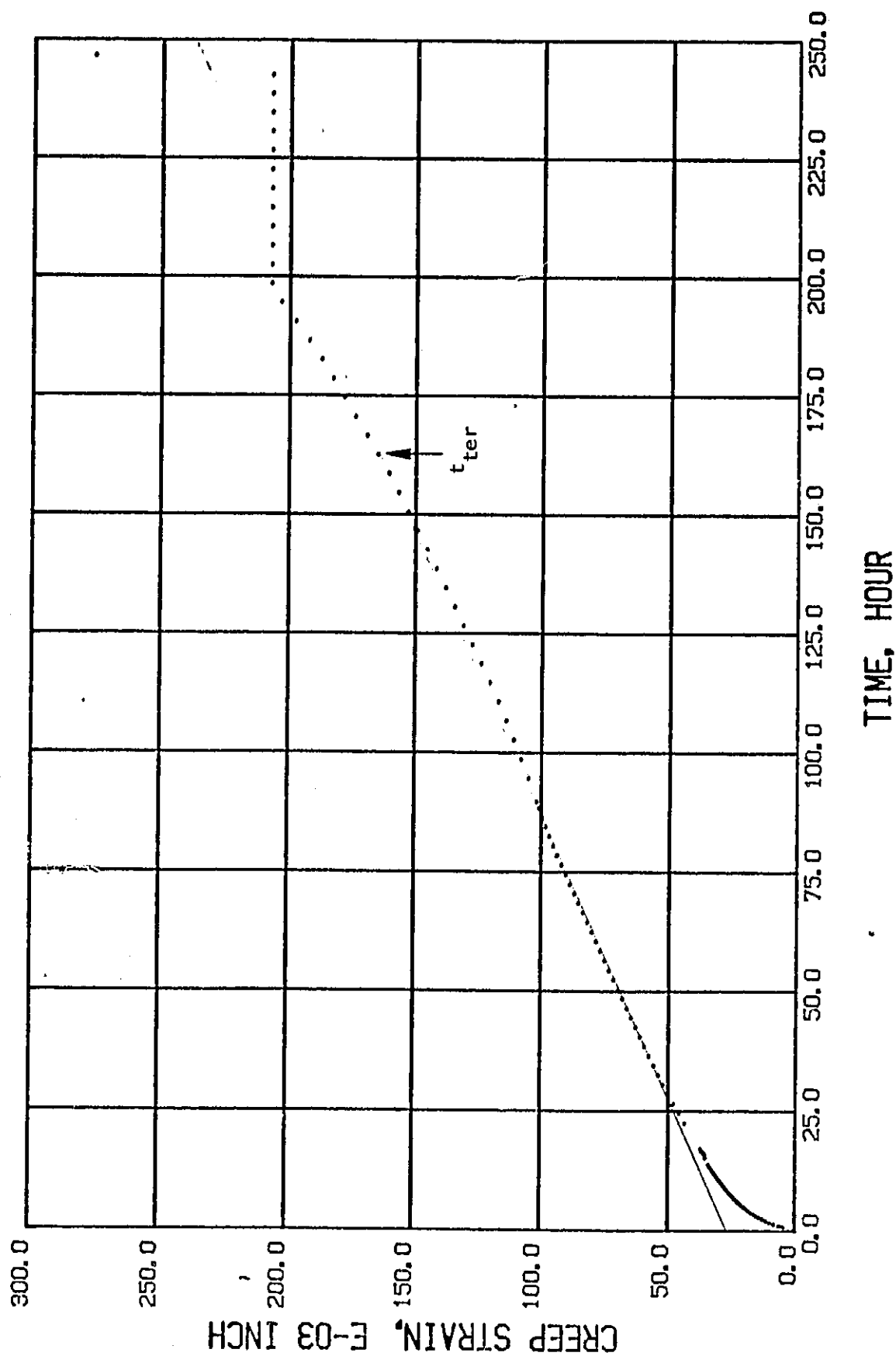
Figure 17. Creep strain-time curve for HS-31 tested at 760°C in 15 MPa H_2. Complete curve, can be used to obtain time to onset of tertiary creep.

IITRI-M06116-3

APPENDIX A

INITIAL LOAD CALCULATIONS

Total load, P (N,1bf) primarily depends on the selected initial stress, σ (MPa, ksi) and the specimen initial cross-sectional area, A (mm^2, in.^{2}) i.e.,

$$P = A\sigma \qquad (A1)$$

The load (P) is obtained by placing P/10 on the pan at the end of a loading arm of ratio 10:1. However, several adjustments to P are made before the modified load is placed on the pan at the arm-end. These adjustments are related to the following factors:

1. Unbalanced weight of the loading arm, supporting strap, and pan

2. Load due to internal pressure acting on the pullwire cross-sectional area and a function of the pullwire diameter

3. Frictional force between the Teflon seal surface and the pullwire surface. This force depends on the coefficient of friction f, and the total normal force on the pullwire.

Of these three items, items 1 and 2 lessen the total weights to be placed on the pan and item 3 must add to it. Typical calculations for two pullwires are shown in Table A-1.

In summary, the net load to be placed on the pan at the end of the lever arm is given by

$$P_{net} = \frac{1}{10} \left\{ \begin{array}{l} \text{P minus Unbalanced load (item 1) minus} \\ \text{Pressure load (item 2) plus} \\ \text{Friction load (item 3)} \end{array} \right\} \qquad (A2)$$

For example, an initial stress of 235 MPa, a typical cast specimen, internal pressure of 15 MPa, a pullwire of 2.03 mm diameter, and an f value of 0.05 will give the following values:

$$P = 235 \text{ MPa} \times 7.92 \text{ mm}^2 \quad = \quad 1860 \text{ N} (418.2 \text{ lbf})$$

Unbalanced load (item 1) = 214 N (48 lbf), constant

Pressure load (item 2) = 48.6 N (10.9 lbf)

Friction load (item 3) = 24.3 N (5.5 lbf) for f = 0.05
14.6 N (2.2 lbf) for f = 0.03

Thus, P_{net} = 1/10 [1860 - 214 - 48.6 + 24.3] = 164 N (36.4 lbf) for f = 0.05

or = 1/10 [1860 - 214 - 48.6 + 14.6] = 161 N (36.2 lbf) for f = 0.03

A mass of 36.4 lb placed on the pan will generate the required initial stress of 235 MPa. If, however, the friction coefficient is less than 0.05, then the applied stress will be higher by about 1 to 2% and vice versa. From test H14 onwards, correction for friction force (with f = 0.05) is included in the initial stress calculations.

It is to be noted that both the internal pressure load and the friction force load are functions of pullwire diameter (and they are opposing forces), and a reduction in diameter lowers both the forces. Pullwire surface is specially polished with 600 grit paper to reduce friction. Internal pressure fluctuation is well within ±2%, and this load thus remains within ±2%. Thus, the overall accuracy of initial stress with or without friction force adjustment can be said to be about <1 to 2%, though the equipment sensor sensitivities are significantly better than ±1%.

TABLE A-1. LOAD FACTORS AFFECTING THE TOTAL LOAD

Item	Remarks
1. Unbalanced weight of the arm, strap, and pan	214 N (48 lbf). Measured in two different ways--through strain gage on pullrod and by a sensitive spring balance.

2. Load due to internal pressure

Internal pressure, 15 MPa (2175 psi)

Pullwire dia		Pullwire area load			
mm	in.	mm^2	10^{-3} in.^{2}	N	lbf
2.03	0.080	3.24	5.03	48.6	10.9
1.60	0.063	2.01	3.12	30.2	6.8

3. Load due to Teflon-stainless steel friction

Seal thickness, 5.08 mm (0.2 in.)

Pullwire dia		Pullwire surface area in contact with seal		Total normal load = pressure x area	
mm	in.	mm^2	10^{-3} in.^{2}	N	lbf
2.03	0.080	32.5	50.3	485	109
1.60	0.063	25.5	39.6	383	86

Friction coefficient	Frictional force, N (lbf) for wire diameter,	
	2.03 mm	1.60 mm
0.03	14.6 (3.3)	11.5 (2.6)
0.05	24.3 (5.5)	19.2 (4.3)

IITRI-M06116-3

APPENDIX B

STRAIN DETECTION USING INTERNAL AND EXTERNAL MEASUREMENT INSTRUMENTS

Sensitive capacitance-type transducers mounted inside the pressure vessel are the primary measuring equipment. These measure strain to 0.25 µm (±10 µin.). Occasionally, this sensitive equipment was observed to get stuck because of minute internal misalignments; when this happens, all strain information can be lost. Realizing the problem from test H14, external dial micrometers were mounted on the loading arm. The dial micrometers can be read to an accuracy of 5 µm (±200 µin.). At the location of mounting, a magnification of about 8 is obtained because of the lever ratio, thus improving the accuracy of the microm-eter measurement to 0.63 µm (±25 µin.), almost within a factor of 2 of the sensitive transducer.

During test H14, both the micrometer and transducer readings were compared and they agreed well. A plot of these readings for SA-F11 up to 445 h is shown in Fig. B-1.

Curve A shows the transducer extension in 25 µm (10^{-3} in.) units. In curve B, the actual dial micrometer values are plotted in 25 µm (10^{-3} in.) units. And, in curve C, the data from curve B were reduced by a factor of 7.8 which is the lever arm ratio at the point on the loading arm where the dial micrometer was set in position. The lateral displacement between curves A and C indicates the difference in the initial setting values. The essential simi-larity between the curves provides the excellent agreement and reliability of the two measuring techniques with the external micrometer performing a continu-ous check on the internal transducer. It is to be noted that in most of the pressure creep experiments reported in the literature, the difficulties of internal strain measurement were avoided by the experimenters by solely relying on external measurements.
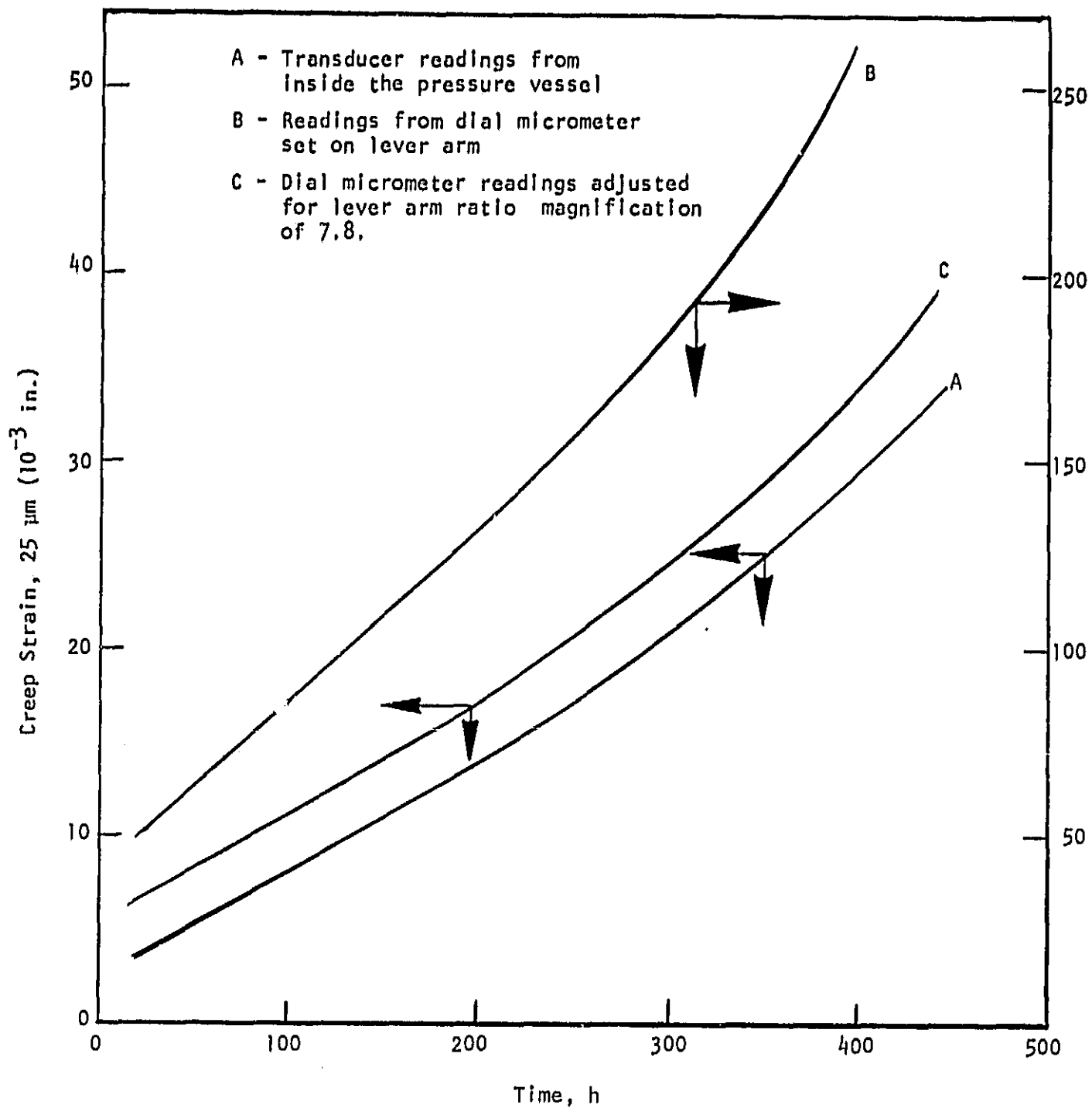
Figure B-1.   *Creep strain measurements for alloy SA-Fll at 760°C in 15 MPa H_2 (test H14).*

IITRI-M06116-3

MONTHLY CONTRACTOR FINANCIAL MANAGEMENT PERFORMANCE ANALYSIS REPORT
NATIONAL AERONAUTICS AND SPACE ADMINISTRATION

Form Approved
Budget Bureau No. 104-R0011

REPORT AS OF: 12/31/82 — 18 days

TO:
NASA-Lewis Research Center

FROM:
IIT Research Institute
10 West 35th Street
Chicago, Illinois 60616

a. TYPE: CPFF

CONTRACT NO. AND LATEST DETERMINED AUTHORIZATION NO.
DEN 3-303

b. DESCRIPTION OF CONTRACT:
Creep-Rupture Behavior of Iron Superalloys in High Pressure Hydrogen

AUTH. COSTS. REP. (Approved)
L.A. Hoornbeek [signature] 3/11/83

COSTS: $ 116,772
FEE: $ 8,174
FUND LIMITATION: $

REPORTING CATEGORY	PLANNED VALUE OF WORK SCHEDULED	ACCOMPLISHED	ACTUAL COSTS HOURS	COST/HOURS	SCHEDULE	VARIANCE COST/HOURS	CONTRACTOR'S ESTIMATED FINAL COST		1*	2	3	4	5	6	7	8	9	10	11	12	% TECH. COMPLETED
Task I – Material Preparation for H₂ Creep-Rupture Testing							Plan															100
							Actual															
Task II – Creep-Rupture Testing in High-Pressure H₂							Plan															30
							Actual															
Task III – Analysis of Data							Plan															15
							Actual															
Task IV – Reporting Requirements							Plan															20
							Actual															

* 4 week periods

1	12/07/82 – 12/31/82	
2	1/01/83 – 1/28/83	
3	1/29/83 – 2/25/83	
4	2/26/83 – 3/25/83	9/30/83: Final Draft 9/07/83
5	3/26/83 – 4/22/83	10/01/83 – 10/28/83: Approved Final 10/22/83
6	4/23/83 – 5/13/83	
7	5/14/83 – 6/10/83	
8	6/11/83 – 7/08/83	
9	7/09/83 – 8/05/83	
10	8/06/83 – 9/02/83	
11	9/03/83 – 9/30/83	
12	10/01/83 – 10/28/83	

NASA FORM 533P SEP 71

DATA APPROVED

37

I1TRI-M06116-3

The monthly and quarterly distribution lists for subject contract are as follows:

	No. of Copies of Reports		
	Financial Report	Technical Monthly	Narrative Quarterly
NASA-Lewis Research Center Attn:			
Commercial Accounts, M.S. 500-303	1		
TU Office, M.S. 3-19			1
R. H. Titran, M.S. 49-1	1	2	2
J. R. Stephens, M.S. 49-1		1	1
S. J. Grisaffe, M.S. 49-1		1	1
T. P. Burke, M.S. 501-11	1		
H. Bankaitis, M.S. 500-211		1	1
W. A. Tomazic, M.S. 500-215		1	1
M&S Division Contract File, M.S. 49-1			1
R. G. Ragsdale, M.S. 500-215			1
Patrick L. Sutton Department of Energy MS 5H-039 Forrestal Building Washington, DC 20545			1
G. Mannella, Director, Stirling Engine Division M.T.I. 968 Albany-Shaker Road Latham, NY 12110			1
Mr. Sten Holgersson United Stirling Research Laboratories ·FACK-201-10 Malmo, 1 Sweden			1
Floyd G. Larson Air-Research Casting Co. 19800 Van Ness Avenue Torrance, CA 90509		1	1